Space Shuttle Entry Longitudinal Aerodynamic Comparisons of Flight 2 with Preflight Predictions

Paul O. Romere* and James C. Young†
NASA Johnson Space Center, Houston, Texas

The Space Shuttle Orbiter flight test program has required the aerodynamicist to take a new approach in determining flight characteristics. A conventional flight test program, where more severe flight conditions are slowly and cautiously approached, was not possible with the Orbiter. On the first two orbital flights, the Orbiter entered the atmosphere at approximately Mach 29 and decelerated through the Mach range (the subsonic portion of flight had also been flown by another Orbiter vehicle during the approach and landing test program). Certification for these flights was achieved by an extensive wind-tunnel test and analysis program. The initial series of flights of the Orbiter are heavily instrumented for the purpose of obtaining accurate aerodynamic data. The flight data derived from the entry Mach range provided comparisons between flight data and wind-tunnel-derived predicted data in the areas of both aerodynamic performance and longitudinal trim. The second orbital flight incorporated several maneuvers which were beneficial to the analysis of the hypersonic aerodynamic performance and the hypersonic longitudinal trim.

Nomenclature

A	= area
AEDC	= Arnold Engineering and Development Center
ARC	= Ames Research Center
b	= wingspan
C'	= proportionality factor for the linear viscosity-temperature relationship
Calspan	= Calspan Corporation
C_A	= axial force coefficient
C_m	= pitching moment coefficient
h	= altitude
h/b	= ratio of altitude from fuselage lower trailing edge to wingspan
HST	= hypersonic shock tunnel
HSWT	= high-speed wind tunnel
IML	= interface mold line
LaRC	= Langley Research Center
L_B	= reference body length
L/D	= lift-to-drag ratio
M	= Mach number
MAC	= mean aerodynamic chord
NSWC	= Naval Surface Weapons Center
PUPO	= pullup/pushover
$\bar{q}$	= dynamic pressure
Re	= Reynolds number based on L_B
S_{REF}	= reference area
TWT	= transonic wind tunnel
UPWT	= unitary plan wind tunnel
$\bar{V}'_\infty$	= viscous interaction parameter $= M_\infty \sqrt{C'_\infty / Re}$
X_{CP}/L_B	= center of pressure in body length
α	= angle of attack, deg
δ_{SB}	= speedbrake deflection angle, deg
ϕ	= roll angle, deg
16T	= 16-ft transonic

Subscript

∞	= freestream

Presented as Paper 82-0565 at the AIAA 12th Aerodynamic Testing Conference, Williamsburg, Va., March 22-24, 1982; submitted March 31, 1982; revision received March 14, 1983. This paper is declared a work of the U.S. Government and therefore is in the public domain.

*Aerospace Engineer, Flight Analysis Branch, Systems Engineering Division.

†Aerospace Engineer, Flight Analysis Branch, Systems Engineering Division. Member AIAA.

Introduction

OBTAINING flight test data over a wide range of flight conditions through a traditional graduated flight test program is not economically feasible on a large, unpowered, gliding flight vehicle such as the Space Shuttle Orbiter. Therefore, an extensive wind-tunnel test and analysis program was undetaken to provide a high level of confidence in the aerodynamic predictions. Also, both the approach and landing test program (ALT) and the current orbital flight test program have been severely restricted to account for uncertainties in the predicted data base, thus assuring a minimum task flight test program. The vehicles were extensively instrumented to obtain flight data. This approach resulted in both high-quality flight test data and an extensive wind-tunnel data base. Thus, the aerodynamicist has been given the unique opportunity to compare state-of-the-art prediction techniques with flight data over an extensive range of entry flight conditions.

The Space Shuttle program's first flight, designated Space Transportation System (STS-1), did not contain any specifically designed data extraction maneuvers; however, the second (STS-2) did incorporate many data extraction maneuvers. Several involved pullup/pushover (PUPO) and body flap pulses, which are most useful in the flight data analysis effort towards the steady-state aerodynamic performance, longitudinal trim characteristics, and control surface effectiveness.

This paper presents an overview of the current analyses of the aerodynamic performance, longitudinal trim, and control surface effectiveness which have been conducted using STS-2 flight data results. Those analyses were directed towards comparisons and correlations of flight data and predicted data, with emphasis on those areas in which differences were significant.

Space Shuttle Orbiter Design Characteristics

The physical characteristics of the Space Shuttle Orbiter are illustrated in Fig. 1. The body flap is the predominant longitudinal trim device, while the wing-mounted elevons are used for longitudinal stability and as ailerons for lateral trim and control. The vertical tail consists of the fin and a combination rudder/speedbrake, with the speedbrake providing lift-to-drag ratio modulation during the terminal area energy management and the approach and landing phases of the

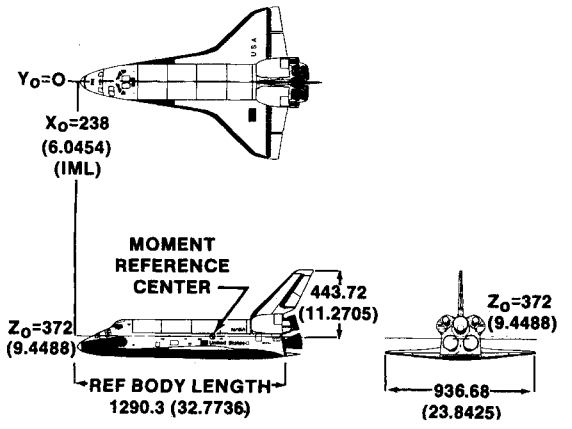

GEOMETRY	COMPONENT	
	WING	VERTICAL TAIL
AREA	2690 FT^2 (249.9092 m^2)	413.25 FT^2 (38.3922 m^2)
SPAN	936.68 (23.8425)	315.72 (8.0193)
ASPECT RATIO	2.265	1.675
TAPER RATIO	0.2	0.404
SWEEP (LE)	81/45 DEG	45 DEG
DIHEDRAL	3.5	— —
INCIDENCE	0.5 DEG	— —
MAC	474.81 (12.0602)	199.81 (5.0752)

NOTE: UNLESS OTHERWISE NOTED, ALL DIMENSIONS ARE IN INCHES (METERS)

Fig. 1 Space Shuttle Orbiter configuration.

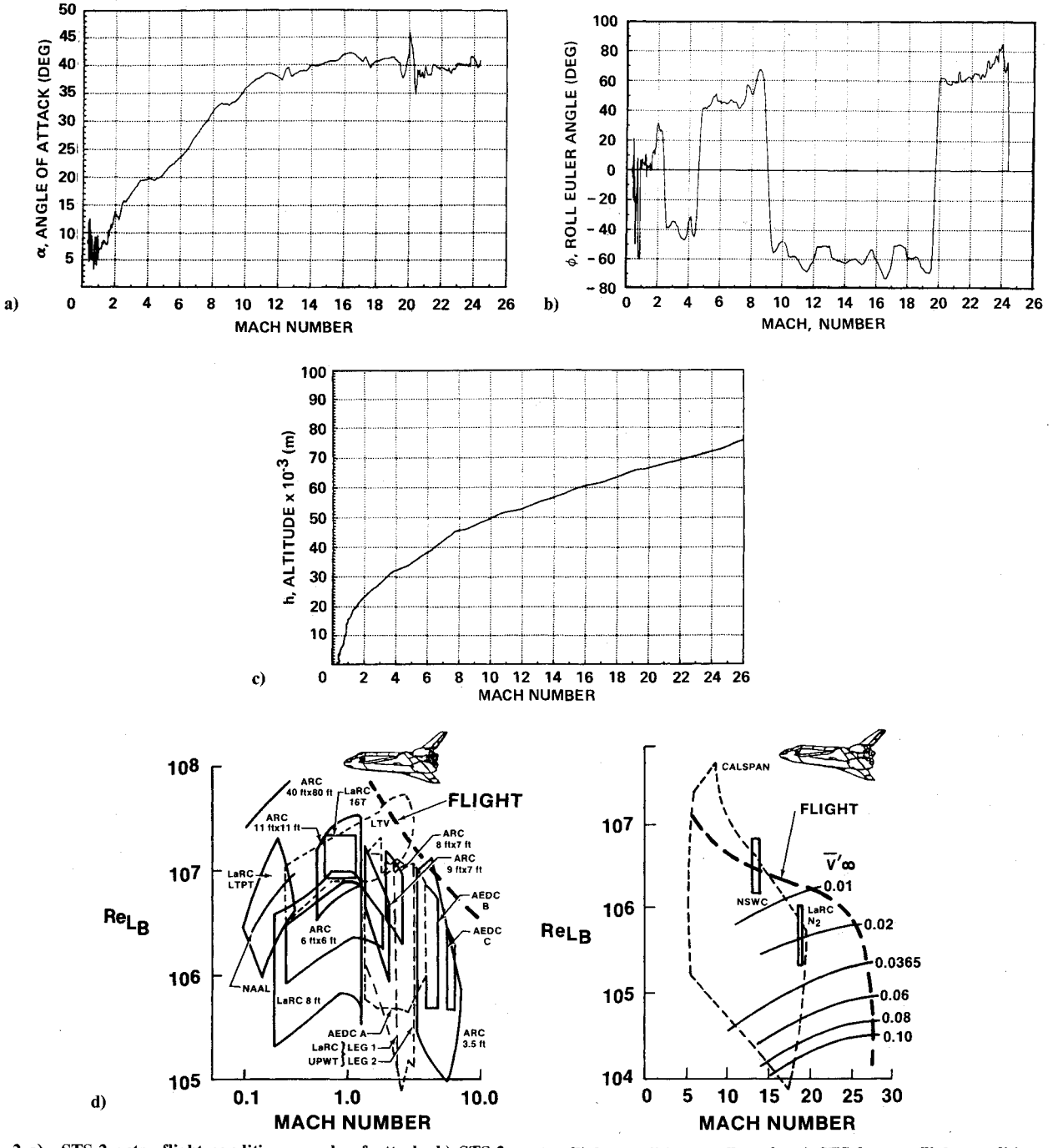

Fig. 2 a) STS-2 entry flight conditions, angle of attack. b) STS-2 entry flight conditions, roll angle. c) STS-3 entry flight conditions, altitude. d) STS-2 entry flight conditions, Reynolds number simulation.

flight. Aft-mounted, sidefiring reaction control jets are used to supplement yaw stability from entry down to Mach 1.0.

The Space Shuttle Orbiter is designed to perform an unpowered, gliding entry from orbit at an angle of attack of 40 deg, which is modulated depending upon crossrange requirements. A gradual pitchdown is initiated at Mach 14 and is completed at Mach 2. From Mach 2 to touchdown, more conventional angles of attack, from 3 to 10 deg, are flown. At the beginning of entry, downrange modulation is achieved by periodically performing roll reversals across the prescribed ground track. STS-2 entry flight conditions are illustrated in Figs. 2a-2d.

Aerodynamically, during the major portions of the flight from entry to touchdown, the vehicle is longitudinally and laterally stable. In certain flight regimes where the vehicle is statically unstable, the stability is artificially provided by the flight control system. The design concept of using a stability augmented flight control system has increased the need to accurately define the aerodynamic characteristics beyond that for a conventional aircraft development program.

Preflight Predictions

The preflight aerodynamic predictions[1] are built on a foundation of 27,000 occupancy hours of wind-tunnel testing. This testing program utilized state-of-the-art facilities, as seen in Table 1.

In general, wind-tunnel data cannot be used directly for prediction; the most valid set of wind-tunnel results must be adjusted for unsimulated conditions. The major adjustments applied to the Space Shuttle wind-tunnel data base involved corrections for nonsimulation of structural deformation, flowfield parameters, and the profile drag due to thermal protection system roughness and minor protuberances. The process of establishing the preflight predictions is discussed subsequently.

A team of aerodynamic experts were called upon to join with the prime contractor in a cooperative effort to establish the most valid set of wind-tunnel tests results. These results were established through a team analysis effort in which the most representative tests were selected, scrutinized for blockage and sting effects, and integrated into an overall data base. The data base was then reviewed and approved by this team of experts.

The traditional freestream Reynolds number was selected for the flowfield scaling parameter below Mach 15, while a viscous interaction parameter ($\bar{V}'_\infty$) was utilized at higher Mach numbers. Since the test facilities were able to provide near-flight Reynolds number simulations over a large Mach number range (as illustrated in Fig. 2d), no corrections to the wind-tunnel results were required. At lower Mach numbers, the traditional adjustments were applied for Reynolds effect on friction drag. Additional adjustments were applied to the profile drag to account for the added roughness of the thermal protection system tiles, and for minor protuberances, which could not be simulated on the wind-tunnel test models.

In the rarefied atmosphere above Mach 15, $\bar{V}'_\infty$ was selected as the scaling parameter. This is appropriate when the boundary-layer thickness becomes significant with respect to the shock standoff distance.[2] The selection was further based upon the assumption that simulation of the shock boundary-layer interaction with the flow on the windward side of the vehicle also provides adequate flight-to-wind-tunnel correlation for the lee side flowfield. An examination of flight conditions with respect to this scaling parameter (Fig. 2d), shows that no adjustments are necessary. The wind-tunnel data were not adjusted for real gas effects.

In general, no attempt was made to obtain a wind-tunnel simulation of the effects of structural deformation on the longitudinal aerodynamics through testing of an aeroelastic or deformed model. Since at higher dynamic pressures ($\bar{q}$) these effects are significant, some adjustment to the wind-tunnel data to account for structural deformation must be made to

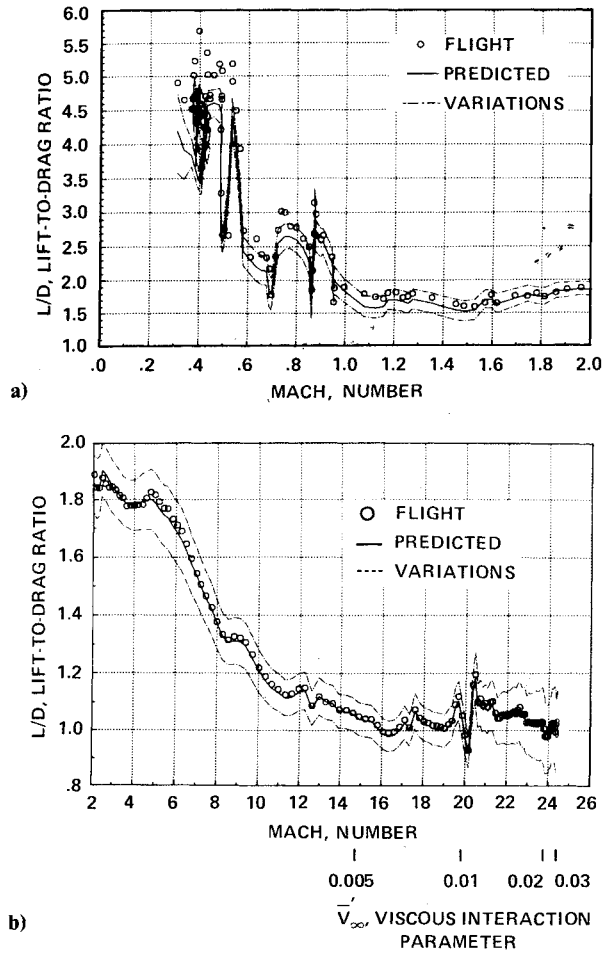

Fig. 3 a) Aerodynamic performance comparison, Mach 0.0 to 2.0. b) Aerodynamic performance comparison, Mach 2.0 to 26.0.

provide adequate estimates of the flight aerodynamics. The approach used to evaluate the aeroelastic effects is unique. These effects were derived using a sensitivity analysis performed with the aid of a structural/aerodynamic analysis program.[3,4] The program was used to stiffen systematically various portions of the vehicle structure and evaluate analytically the effect of the stiffness changes on the aerodynamics. The results indicated that the major longitudinal aeroelastic effects were produced by deformation of the elevon about its hinge line as a result of the aerodynamic hinge moments. The effect was modeled by combining a rotary spring constant, as determined from vehicle loading tests, with wind-tunnel-derived aerodynamic hinge moment characteristics to produce an elastically deformed elevon deflection angle. The elastic elevon angle is subsequently used with the rigid aerodynamic characteristics in determining the vehicle longitudinal aeroelastic characteristics.

As a result of the Space Shuttle program management's desire to desensitize the flight control system with respect to the aerodynamics, uncertainties (defined as variations) were provided for use with the preflight predictions. These variations[1] are based upon historical predicted-to-flight differences of similar configurations and on engineering judgment.

Comparisons of STS-2 Flight to Predicted Data

The aerodynamic analyst is faced with a dilemma in the comparison of preflight predictions and flight data. In wind-tunnel testing, which is the basis of the preflight predictions, the independent parameters are known precisely while the

aerodynamics are questionable. In flight testing, the aerodynamics are known exactly, by definition, but the accuracy of the independent parameters may be in question. To minimize the impact of this dilemma, the aerodynamic comparisons were selected such that errors in the flight-independent parameters are minimized.

Lift-to-drag ratio (L/D) was selected for comparisons of predicted and flight aerodynamic performance since it is independent of flight dynamic pressure ($\bar{q}$). As may be seen in Fig. 3, the preflight predictions agree well with flight L/D above Mach 1. Below Mach 1, the flight exhibited higher L/D than predicted.

At a Mach number of approximately 21 during the STS-2 entry, a pullup/pushover (PUPO) maneuver was executed in which angle of attack varied from 35 to 45 deg. During this maneuver, the only control surface movement involved that of the elevons to drive the vehicle through the angle-of-attack sweep from 35 to 45 deg and back to 37 deg. Figure 4 presents the correlation of flight to predicted L/D for the PUPO. The correlation is excellent, with a maximum difference being approximately 1½%. The predicted variations in this region are approximately 10%.

The longitudinal aerodynamic center of pressure (X_{CP}/L_B), which is also independent of $\bar{q}$, was selected for trim comparisons. For a trimmed vehicle, the longitudinal center of pressure (the imaginary point on the vehicle where the pitching moment is zero) coincides with the center of gravity. Figure 5 presents a comparison of the flight and predicted centers of pressure. As can be seen in Fig. 5b, at Mach numbers above 10, the predicted center of pressure is more aft by 0.7% of the reference body length (1.9% of the mean aerodynamic chord) than the flight data would indicate. For the Mach range of 14-20, differences are outside of predicted variations. In the Mach range where the Reynolds number was simulated ($2.0 \leq M \leq 10$; Fig. 2d), trim was predicted more precisely, even though a unusually high angles of attack between 15 and 30 deg were flown. The predictions for the transonic and subsonic range were less than satisfactory although they were within the predicted variations. The slight difference between flight and predicted in the Mach 2 to 10 range of Fig. 5b was not noted in STS-1 results[5] and can be attributed to a possible uncertainty in the center of gravity location for STS-2.

In addition, axial force coefficient (C_A) comparisons have been made. Two observations can be made from the C_A comparisons of Fig. 6. The underprediction of L/D previously reported was largely influenced by the overprediction of C_A in the same Mach range. Figure 6b indicates that the viscous interaction parameter ($\bar{V}'_\infty$), which is used above Mach 15, was a wise choice of scaling parameters for C_A. The trends of flight-derived and predicted C_A indicate a possible error in determination of the flight angle of attack. Such a bias was not evident in STS-1 comparisons. The higher flight C_A seen at Mach 13 corresponds to a flight control system update which involved an aileron input, possibly causing a control surface induced laminar-to-turbulent boundary-layer transition. The phenomenon is still under investigation.

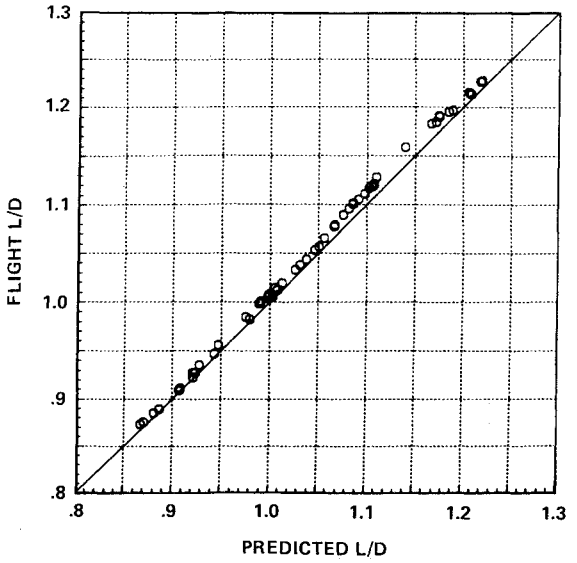

Fig. 4 Correlation of hypersonic lift-to-drag ratio from flight and prediction using a pullup/pushover maneuver.

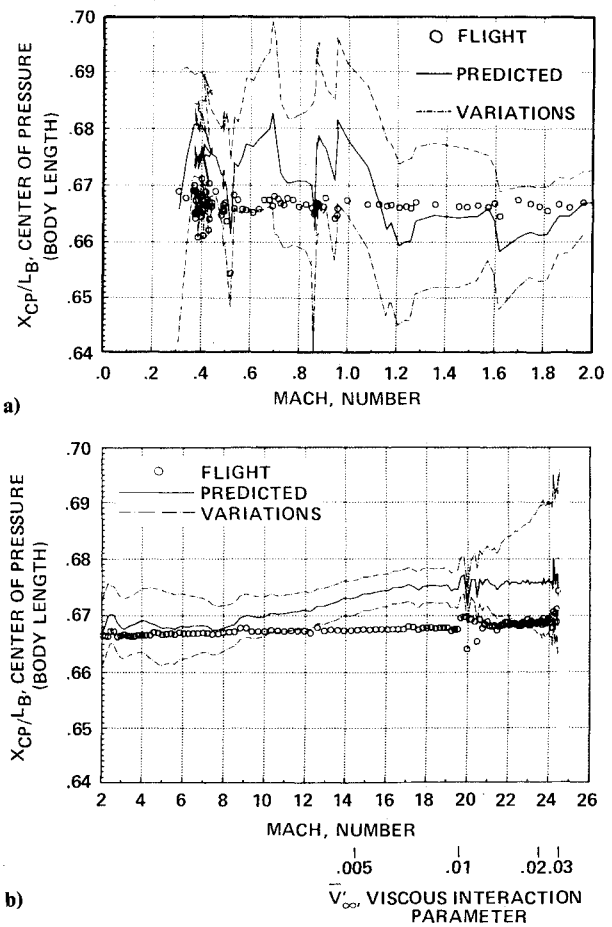

Fig. 5 a) Longitudinal aerodynamic center of pressure location comparison, Mach 0.0 to 2.0. b) Longitudinal aerodynamic center of pressure location comparison, Mach 2.0 to 26.0.

Longitudinal Trim Difference Analysis

Upon examination of the X_{CP}/L_B correlation (Fig. 7) derived from the previously mentioned pullup/pushover maneuver, the data indicated a very good straight line correlation which is parallel to but biased from the perfect correlation line by approximately 0.0075. The data, being essentially parallel to the perfect correlation line, indicate that the effects of angle of attack and elevon effectiveness are as predicted, and the bias is probably the result of not correctly predicting the basic vehicle pitching moment or underprediction of the body flap by approximately 50%. Illustrated in Fig. 8 are the X_{CP}/L_B correlations of data taken during body flap pulse maneuvers at Mach numbers of approximately 21, 17, and 12.5. During those maneuvers the angle of attack was near constant with only the body flap and elevons moving.

Each body flap maneuver of Fig. 8 illustrated a generally straight line correlation which was parallel to the perfect correlation line and biased in the same manner as the PUPO maneuver. The inference here is that both the body flap and

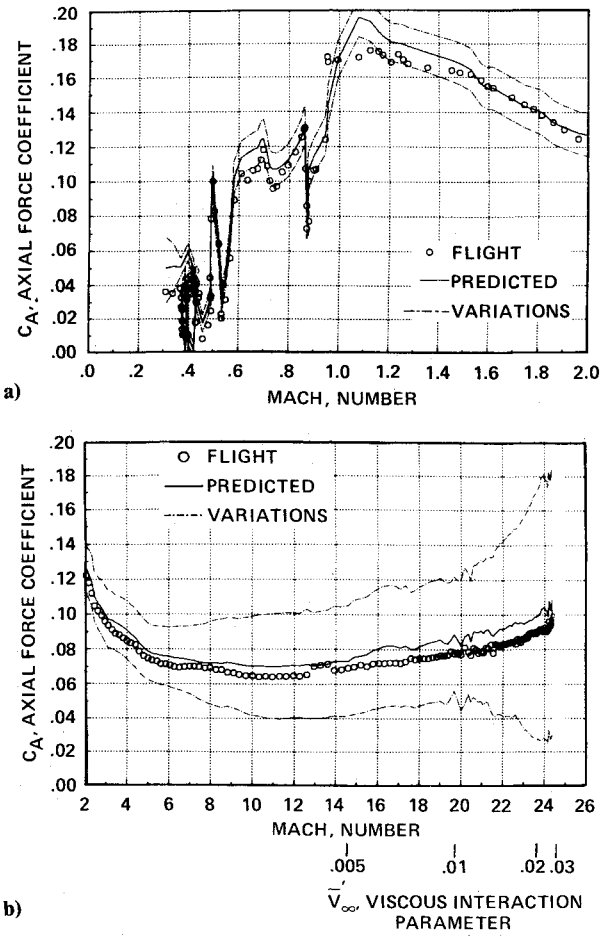

Fig. 6 a) Axial force coefficient comparison, Mach 0.0 to 2.0. b) Axial force coefficient comparison, Mach 2.0 to 26.0.

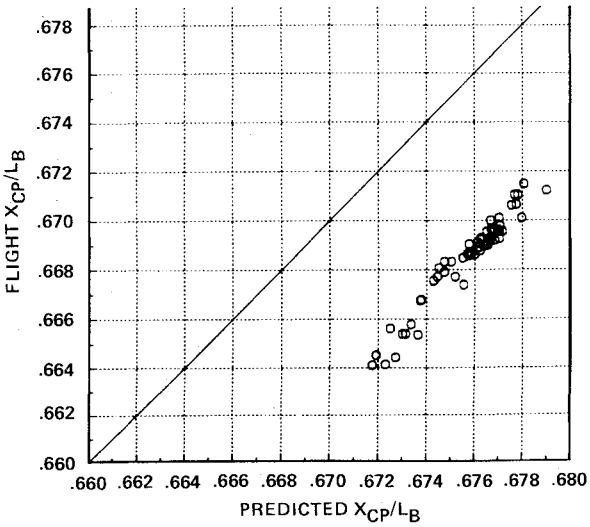

Fig. 7 Correlation of hypersonic longitudinal aerodynamic center of pressure data from flight and prediction using a pullup/pushover maneuver.

elevon effectiveness are as predicted. The ratio of the change in elevon deflection to the change in body flap deflection from the flight data is as was predicted. This lends additional strength to the inference that both body flap and elevon effectiveness were well predicted. Therefore, one would conclude the most probable cause for the hypersonic trim discrepancy would be an error in the predicted basic pitching moment of the vehicle. The wind-tunnel results were re-

Table 1 Shuttle wind-tunnel utilization summary

Test identification	Facility	Model scale
Transonic		
0A145A	ARC 11×11 ft	0.05
0A270A	LaRC 16T	0.05
0A270B	LaRC 16T	0.02
LA70	Calspan 8 ft	0.015
LA76	LTV 4×4 HSWT	0.015
LA77	ARC 11×11 ft	0.015
LA111	LaRC 8 ft TWT	0.015
LA115	LaRC 8 ft TWT	0.015
Supersonic		
0A145B	ARC 9×7 ft	0.05
0A145C	ARC 8×7 ft	0.05
0A209	AEDC "A"	0.02
LA63A	LaRC UPWT-1	0.015
LA63B	LaRC UPWT-2	0.015
LA75	LaRC UPWT-2	0.015
LA76	LTV 4×4 ft HSWT	0.015
LA101	LaRC UPWT-1	0.015
LA110	LaRC UPWT-1	0.015
LA114	LaRC UPWT-2	0.02
LA125	LaRC UPWT-2	0.02
LA131	LaRC UPWT-2	0.02
LA144	LTV 4×4 ft	0.02
0A258	AEDC "B"	0.02
0A259	AEDC "B"	0.01
0A257	LaRC 20 in.	0.01
Hypersonic		
0A113	Calspan HST (48 in.)	0.01
0A171	NSWC Tunnel 9	0.02

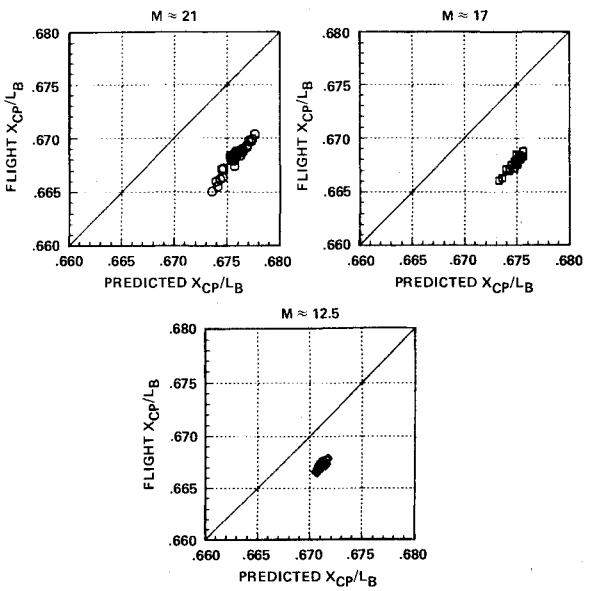

Fig. 8 Correlations of hypersonic longitudinal aerodynamic center of pressure data from flight and prediction using body flap pulse maneuvers.

examined to insure that no data were overlooked which would better reflect the flight data results. None were found.

One must conclude that the proper scaling was not realized for the hypersonic trim characteristics, either because the scaling parameter was improperly selected or because the test facilities were not capable of reproducing the proper environment. In that the discrepancy is indicated to result from a basic pitching moment error, the probable cause is due to the test facilities not reproducing the proper environment, namely, to simulate real gas effects. Aware that real gas

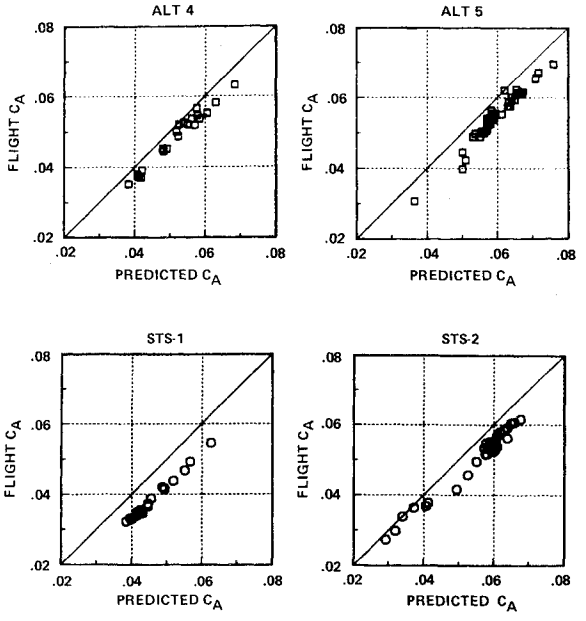

Fig. 9 Correlations of subsonic axial force coefficient data from flight and prediction.

effects can not be simulated in ground-based test facilities, real gas effects, which primarily affect the pitching moment, were analytically derived and included in the predicted data base. However, due to the uncertainties associated with the analytically derived effects, they were applied to the predicted moment uncertainties, or variations mentioned previously. It should be noted that the analytically derived real gas effects do give the correct trends and approximate magnitudes required to better predict the flight characteristics.

Subsonic Performance Difference Analysis

As a result of the discrepancy between flight performance and predicted performance in the subsonic range, the Space Shuttle Orbiter was analyzed with respect to drag and speedbrake effectiveness. Data from flights 4 and 5 of the approach and landing test program (ALT 4 and ALT 5) and STS-1 and STS-2 were used. The drag analysis was centered on the axial force coefficient and included only the flight data taken with a speedbrake deflection of less than 30 deg, with the landing gear retracted, and above the region of ground effects (i.e., $h/b>1.5$). Correlation plots of flight to predicted data are presented in Fig. 9 and indicate an overprediction of C_A by a constant 40 counts ($C_A=0.004$) for all flight data sets, with the exception of that for the final data reduction of STS-1, which indicates an overprediction of approximately 70 counts. No explanation for the STS-1 discrepancy is available at the present time. A significant improvement in the correlations resulted from correcting the predicted profile drag by -40 counts (see Fig. 10). The data presented in Figs. 9 and 10 are for Mach ≈ 0.47 to 0.5.

For the analysis of speedbrake effectiveness, flight test data were selected where body flap deflection was approximately 0 deg, and the speedbrake was swept through a large deflection range. The flight data were then corrected to an angle of attack of 5 deg and an elevon deflection of 5 deg through the use of the coefficient slopes as determined from the predicted data base. The resultant effectiveness with respect to axial force coefficient is presented in Fig. 11 as an increment about the baseline speedbrake deflection of 25 deg. For STS-1 and STS-2, the effectiveness was underpredicted by approximately 60 counts at a 55-deg speedbrake deflection angle. Results from ALT 4 and ALT 5 do not indicate this underprediction. Resolution of this flight data inconsistency will require further analysis.

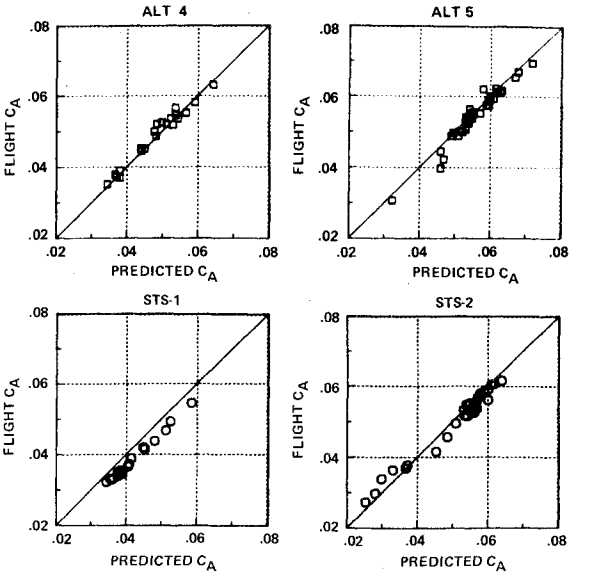

Fig. 10 Correlations of subsonic axial force coefficient data from flight and prediction corrected by -40 counts.

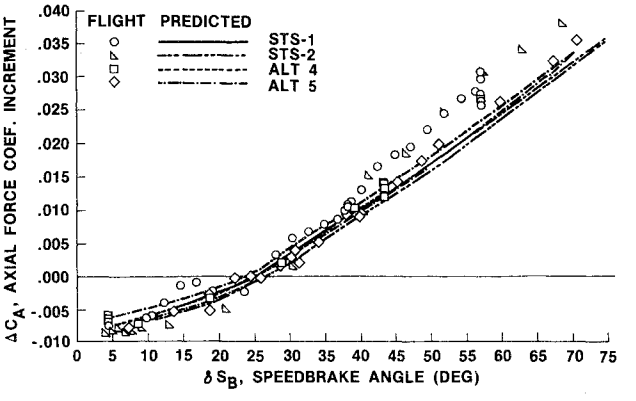

Fig. 11 Subsonic axial force coefficient increment due to speedbrake deflection.

Concluding Remarks

The completion of the first and second flights of the Space Shuttle Orbiter has given aerodynamicists the first opportunity to test their prediction skills over diverse flight conditions. The performance predictions were in excellent agreement with flight performance above Mach 1; however, drag was overpredicted at the subsonic Mach numbers.

The trim characteristics were predicted adequately in the Mach range of 2 to 10; however, above Mach 10 and below Mach 2, the predictions were less than satisfactory. Analysis results of the STS-2 maneuvers during entry indicate the hypersonic trim discrepancy is due to an error in prediction of the basic vehicle pitching moment and not an error in prediction of the elevon and body flap effectiveness.

References

[1] *Aerodynamic Design Data Book, Volume 1, Orbiter Vehicle 102,* SD72-SH-0060, Vol. 1L, Revision 5, Space Division, Rockwell International, Oct. 1978.

[2] Cox, R.N. and Crabtree, L.F., *Elements of Hypersonic Aerodynamics,* Academic Press, New York, 1965.

[3] "Aerodynamic Preliminary Analysis System, Part I—Theory," NASA CR 145284, April 1978.

[4] "Aerodynamic Preliminary Analysis System, Part II—User's Manual and Program Description," NASA CR145300, April 1978.

[5] Young, J.C., Perez, L.F., Romere, P.O., and Kanipe, D.B., "Space Shuttle Entry Aerodynamic Comparisons of Flight 1 with Preflight Predictions," AIAA Paper 81-2476, Las Vegas, Nev., Nov. 1981.